

Modelling of Large Size Electrolyzer for Electrical Grid Stability Studies in Real Time Digital Simulation

P.Ayivor¹, J.Torres¹ and M.A.M.M. van der Meijden^{1,2}

¹Delft University of Technology, Delft, The Netherlands ²TenneT TSO B. V, Arnhem, The Netherlands
p.k.s.ayivor@student.tudelft.nl, j.l.ruedatorres@tudelft.nl,
mart.vander.meijden@tennet.eu

R. van der Pluijm³ and B.Stouwie³

³EnergyStock B.V, Groningen, The Netherlands.

Abstract— This paper provides an overview on implementing practical models of large scale electrolyzers (>1MW) for real time digital simulation. The search for new sources of ancillary services has aroused considerable interest in the use of large scale electrolyzers for power system ancillary services. As the number of large scale electrolyzers is projected to grow, it is important that the dynamics of these plants are well understood in order to integrate them successfully. In line with this objective, suitable models must be developed to aid studies of grid dynamics with electrolyzers configured as sources of ancillary services. To illustrate the feasibility of creating such models, a case study is built on a MW-scale plant connected to an infinite grid. Real time simulations are performed by using a real-time digital simulation (RTDS) platform to investigate the response of the electrolyser model to basic step commands. The results show that a generic scalable model of large scale electrolyzers in RTDS can replicate fairly accurately the response of a real electrolyser.

Keywords- RTDS, model, large scale, electrolyser

I. INTRODUCTION

The growing interest in hydrogen, as an energy carrier, has been significant in the recent years due to increased awareness of climate change. Hydrogen has been identified as a clean and flexible energy carrier that can be used to provide both power and heat across multiple end-use sectors [1]. According to [2], hydrogen will play an important role in the future multi-energy system. Currently approximately 4% of hydrogen is produced from electrolysis globally [3] and this amount is growing as new Power-to-Gas plants are commissioned. For instance, it is estimated that 270,000 tons of hydrogen will be produced in Northern Netherlands alone, between 2017 and 2030 to support multiple sectors (industry, mobility, electricity generation, heating etc.) [2]. This projected increase in demand for hydrogen for the various sectors will be achieved with several megawatts of electrolyzer capacity [2]. Power-to-Gas enables the power grid operator to integrate large amounts of surplus renewable generation when it is not needed and enables options to store and transport this energy as renewable hydrogen. Power-to-Gas provides unparalleled scale of energy storage and enhances system flexibility. The scale of pilot Power-to-Gas projects built to date range from 100 kW to 6 MW (with the majority less than 1 MW), the capacity

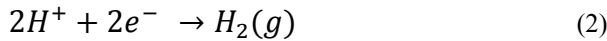
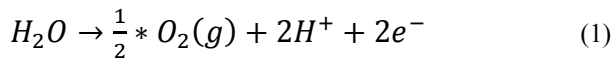
required for commercial projects will likely be large scale with capacities in the range of tens to hundreds of MW [3]. The reason for this is the massive scale of energy storage required. For jurisdictions with a high penetration of Variable Renewable Energy Source (VRES), the energy storage requirement is in GWh, and the size of power ramps from VRES output will be in the order of hundreds of megawatts [3]. Integrating large scale (>1MW) electrolyzers requires a good understanding of their interactions with existing grid. This understanding can be facilitated with good models of the real systems. Modeling and simulation of large scale electrolyzers in a real-time simulation environment (such as Real Time Digital Simulator -RTDS) presents a cost effective and low risk method to aid the study of potential effects of large scale electrolyzer integration. The current challenge of model concepts available in current literature is that large scale versions (>1MW) are not available [4]. The key contribution of the paper is the demonstration of the feasibility of creating generic and scalable models of large scale electrolyzers. The paper provides an overview of main electrolyzer system components, the mathematical foundations of these components and a demonstration of how they are implemented with existing library components in RSCAD software of RTDS. Focus is on the basic building block of large scale electrolyzers; i.e. the components of a 1MW proton exchange membrane (PEM) electrolyser plant. The method to scale the 1MW model to higher capacities (e.g. 300MW) is also demonstrated. Finally the responses of the model to ramp up and ramp down step commands are also examined and verified with real responses from a PEM electrolyzer. A case study, built upon a high voltage grid model connected to an electrolyser via a step down transformer, is used to demonstrate the response of the 1MW Power to Gas Plant to step changes in demand set points.

The paper is organized as follows: Section II provides an overview of the PEM electrolyser system, section III examines the PEM stack and how the RSCAD model is developed. Similarly sections IV and V explore the power conversion system and balance of plant component modeling respectively. Section VI looks at the performance of the RSCAD model and compares it with the response

from a real electrolyser. Section VII demonstrates the scaling approach. Conclusions from the simulations and the focus of future research are summarized in section VIII.

II. OVERVIEW OF PEM ELECTROLYSER SYSTEM

Hydrogen can be produced by water electrolysis, steam reforming, biological processes or photochemical reactions [6]. The production of hydrogen in this paper however, is limited to the electrolysis of water. Water electrolysis is an electrochemical process in which electricity is applied to split water into hydrogen and oxygen. In the first part of the reaction, water is oxidized into protons, electrons and oxygen. The produced oxygen is transported and removed from the cell. Protons from the oxygen evolution reaction (OER) at the anode are transported through a diaphragm/membrane to the cathode and are reduced to molecular hydrogen in the hydrogen evolution reaction (HER) described by (2). The overall electrolysis reaction is the sum of the two electrochemical half reactions, which takes place at the electrodes in an acidic environment according to the following equations:



These are the basic reactions that govern the electrolysis reaction. Electrolysers are devices that carry out the water electrolysis process. According to [5] four types of electrolysers exist:

- PEM electrolysers
- Alkaline electrolysers
- Solid Oxide electrolysers (SOE)
- Anion exchange membrane (AEM)

Currently, both PEM and alkaline electrolyzers are commercially available. Electrolysis based on AEM has a limited range of products, whereas SOE technology is at the early stage of development. Among the electrolysis technologies, alkaline electrolysis is the most mature. Although alkaline technology is also well suited to Power-to-Gas for smaller-scale projects, there are some clear advantages for using PEM technology for large-scale commercial projects. PEM electrolysis, though in its initial commercial phase, shows significant promise for future applications [3]. PEM electrolyzers operate at significantly higher current densities, meaning significant stack volume reduction compared with alkaline technology. This enables significantly smaller Power-to-Gas plant footprints with PEM technology. Today, the capital cost per MW and the efficiency (percentage of electrical energy converted to hydrogen) of most PEM electrolyzers is similar to that of alkaline electrolysers [3]. While alkaline electrolysis is a mature technology that has reached a performance plateau, PEM electrolysis technology is at nascent stage with plenty of room for more development to increase power density, efficiency, and cost. PEM electrolyzer technology holds the highest promise for the lowest capital cost along with higher power densities, smaller footprint, larger dynamic range, and a scalable design [3]. The models developed in this paper are therefore based on the PEM technology.

Figure 1 depicts the general PEM electrolyser system layout. This diagram is not a general standard however it captures the relevant components and subsystems. According to [5] an electrolysis system is made up of three layers; the PEM stack layer which is the unit within which the chemical reaction takes place, the PEM module layer which includes the stack as well as peripheral components to support stack operation (i.e. supply of reactants and removal of products) and the system layer which comprises the module layer and other auxiliary subsystems that vary based on the installation site and application. Examples of auxiliary subsystems in the system layer are water purification systems, buffer gas reservoirs, hydrogen purification systems etc.

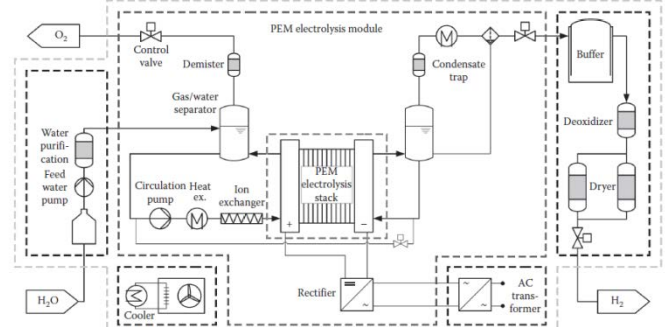


Fig 1: General system layout of an electrolyser showing the PEM stack and balance of plant components (controls not shown). Extracted from [13]

The PEM stack is the main component within which the production of hydrogen and oxygen takes place. It must be noted however that the operation of the stack is only feasible with the support of other subsystems. The generic model proposed by this paper models the PEM system at the module layer, thus the Balance of Plant (BoP) components which support the operation of the stack such as feedwater and circulation pumps are modelled. The multitude of changes required for each installation and site make it difficult to capture the system layer in a generic model. The key components whose electrical response the generic RSCAD model emulates are the PEM stack, the power conversion system (rectifier, DC-DC converter and main transformer) and the balance of plant components namely the circulation pump, cooling system and electronic loads such as the control system. The chemical reaction within the PEM stack is not modelled.

III. PEM STACK MODEL AND REPRESENTATIONS IN RSCAD

Electrolysis requires a direct current (DC) source to provide the electrical power to drive the process. This section shows modelling of a PEM (proton exchange membrane) electrolyzer stack within the module layer. The main losses in such PEM electrolyzer stack are also modelled. It must be noted that several parameters in the model are difficult to fix, because they vary for each electrolyser device and also because of challenges with obtaining proprietary information. However practical ranges for these parameters are obtained from available literature. In order to use these models, their parameters have to be estimated. Results of experimental identification techniques such as Electrochemical Impedance Spectroscopy can be converted to an equivalent circuit [6] [7]. Another option is to obtain parameters from manufactures' data. The model of the PEM

module comprises three main parts: the PEM stack, Power Conversion System and Balance of Plant components. The input DC voltage applied to a PEM cell must overcome the reversible voltage in order to trigger the chemical reaction of water splitting into oxygen and hydrogen. In practice the cells are electrically connected in series to achieve the required hydrogen output, therefore the total voltage is a sum of the reversible voltage and contributions of the various over potentials for each cell. Therefore the voltage applied to the cell V_{cell} can be written as:

$$V_{cell} = V_{rev} + V_{act} + V_{diff} + V_{bub} + V_{ohm} \quad (3)$$

Where V_{rev} is the reversible potential, V_{act} , V_{diff} , V_{bub} and V_{ohm} are the activation, diffusion, bubble and ohmic overpotentials respectively. Losses within the PEM stack are modelled as overpotentials. In order to build the steady state electrical model of the PEM cell, the reversible voltage and each overpotential is examined.

A. Reversible voltage

The splitting of water is driven by electrical and thermal energy input [5]. The energy input to the process can be represented mathematically as described in (4). State of the art PEM electrolysis modules operate at low temperatures (<373.15K) implying that the larger part of energy input is obtained from electrical energy. The total energy demand to split water molecules decreases slightly with increasing temperature until the boiling point where water gets in its gaseous state and total energy demand increases again.[5]. Assuming a lossless electrolysis process, the potential difference at the electrodes of the cell is called the reversible cell voltage. This voltage is the minimum voltage required to drive the process assuming the requisite thermal input is present. It can be calculated by:

$$V_{rev} = \frac{\Delta G_R}{z \cdot F} = 1.229V \quad (4)$$

Where ΔG_R is the Gibbs free energy of the reaction defined as 236.483[kJ per mol], F is the Faraday constant 96,485 [Coulombs per mol] and z is the amount of charges (electrons) transferred during the reaction (i.e. 2). However without external thermal input, the voltage required to activate the process is higher because of a higher energy requirement for the reaction. This voltage is known as the thermoneutral voltage at standard state (defined as temperature of 25 degrees Celsius and 1 atmosphere pressure).

$$V_{th} = \frac{\Delta H_R}{z \cdot F} = 1.481V \quad (5)$$

Where ΔH_R is the enthalpy of reaction for liquid water defined as -285.83 [kJ per mol] under standard conditions. This reversible voltage can be obtained for various levels of temperature and pressure using the (6), the Nernst equation.

$$V_{rev} = V_0 + \frac{R \cdot T}{(2 \cdot F)} * \ln \left(\frac{P_{H_2} \cdot P_{O_2}^{0.5}}{a_{H_2O}} \right) \quad (6)$$

Where $R = 8,314 \text{ J/mol Kelvin}$, $F = 96 \text{ 487 Coulombs per mol}$, $V_0 = 1.23 \text{ [V]}$, $a_{H_2O} = 1$ (for liquid water), P_{H_2} and P_{O_2} are universal gas constant, Faraday constant, standard reversible voltage, water activity the partial pressures (in Megapascals) of hydrogen and oxygen respectively. It can be seen that the reversible voltage decreases with increasing temperature. This is the

theoretical open cell voltage when there is no current flowing through the PEM stack.

B. Losses in a PEM electrolysis cell

As shown in (3) and (4), the theoretical open-cell voltage (OCV) for the electrolysis of water is 1.229 V or 1.48 V (without thermal energy input). When current flows through the stack however, the actual voltage for water splitting increases above the OCV value, due to irreversible losses within the cell. There are three major mechanisms that lead to losses in a PEM electrolysis cell: activation losses due to slow electrode reaction kinetics, ohmic losses, and mass transfer losses [5]. The above losses can be further categorised in two categories—the faradaic and the non-faradaic processes. The activation losses are faradaic and are linked to the direct transfer of electrons between redox couples at the interface between the electrode and the electrolyte of the oxygen evolution reaction (OER) and the hydrogen evolution reaction (HER). Non-faradaic losses are those that do not result from the direct transfer of electrons across the electrodes due to electrochemical reaction. The ohmic and mass transport losses are related to non-faradaic loss mechanisms. Ohmic losses are due to resistance to electron flow through the electrodes and cell components as well as resistance to the flow of protons through the membrane and are directly proportional to the amount of current passed through the cell. Mass transport losses are in two main forms: diffusion and bubbles overpotentials. Diffusion losses occur when gas bubble partly block the pores of current collectors and thereby limiting the supply of reactant water to the process, while bubbles over potential result when large gas bubbles shield the active area and reduce catalyst utilization. In electrolyzers the irreversibilities appear in the form of overpotentials or overvoltages that are summed up to the cell potential.

The losses at the anode and cathode are represented by the anodic activation overpotential cathodic activation overpotential respectively. These together form the total activation overpotential. Activation losses are dominant at low current densities [5]. The activation overpotential is caused by the speed of the reactions that occur at the surface of the anode and cathode. A proportion of the voltage supplied is used to drive the chemical reaction that transfers the electrons to or from the electrode. This overpotential is nonlinear, varies with the current and predominates at lower currents. The activation voltage drop equation can be obtained from Butler-Volmer and Tafel laws [17]. The activation overpotential can be rewritten as a function of the current as shown in (7).

$$V_{act} = R \cdot \frac{T}{\alpha \cdot n \cdot F} * \ln \left(\frac{I}{I_0} \right) \quad (7)$$

Where α , n and I_0 are the transfer coefficient, number of electrons transferred and the exchange current respectively. Diffusion losses occur when gas bubbles partially blocks the pores network of current collectors and thereby limiting the supply of reactant water to the active sites, while bubbles overpotential arises when very large gas bubbles shield the electrochemical active area, reducing catalyst utilization. At high current densities (>2mA/cm sq.), the production of bubbles shields the active area and reduces the contact area between the electrode and the electrolyte. This reduces the catalyst utilization and results in an

increase in the local current density and resultant bubbles overpotential. This rise in local current density increases exponentially with increasing current densities [5]. The concentration of fluids (gas and water) and diffusion close to the electrodes influence the value of the current. These changes induce the voltage diffusion drop. The diffusion voltage V_{diff} can be obtained from (8).

$$V_{diff} = R \cdot \frac{T}{\beta \cdot n \cdot F} * \ln \left(1 + \frac{I}{I_{Lim}} \right) \quad (8)$$

Where β , n and I_{Lim} are the constant coefficient, number of electrons transferred and the diffusion limit current respectively. Ohmic losses are due to resistance to electron flow through the electrodes and cell components as well as resistance to the flow of protons through the membrane. It is directly proportional to the amount of current passed through the cell according to Ohm's law. Ohmic loss, modelled by ohmic overpotential, become dominant at mid current densities [5]. The resistance of the polymer membrane is the main cause of ohmic voltage drop. The resistance value is a function of membrane section area, membrane thickness, hydration ratio (=7 dry enough =14 good hydration, =22 bathed) and temperature. Where λ is the membrane hydration ratio.

$$V_{ohm} = \frac{l_m}{A_m \cdot (0.005139 \cdot \lambda + 0.00326) \cdot \exp \left(1267 \left(\frac{1}{303} - \frac{1}{T} \right) \right)} \cdot I \quad (9)$$

C. Equivalent circuit of PEM cell

The electrical response of the PEM stack is characterized by the open cell voltage and overpotentials. The actual cell voltage for water splitting is the sum of the open cell voltage plus, all irreversibilities within the cell. Summing (6), (7), (8) and (9) yields the mathematical model for the PEM electrolysis cell. The model can then be represented by an electrical equivalent circuit which represents the overpotentials with resistances [8]. The charge double layer phenomenon that takes place at the electrode-electrolyte interface is modelled by a capacitance in parallel with the activation and mass transport resistances as shown in Fig 2. According to [8], the above representation of the electrical equivalent is widely used in current literature. This representation using resistances and capacitance is useful for analysis of dynamic behaviour of the electrolyzer. R_{act} ; R_{mass} and R_{ohm} represent

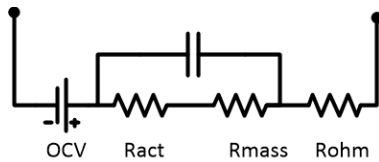


Fig 2: Electrical equivalent of PEM cell showing reversible voltage and overpotentials represented by resistances.

activation, mass transport and ohmic losses respectively. Reversible voltage is represented by fixed DC voltage; OCV. The double layer capacitance of the cell is represented by a capacitor in parallel with the series combination of R_{act} and R_{mass} .

D. Simplified Electrical equivalent circuit

For large scale electrolyzers the model is further reduced based on the following assumptions:

- The mass transfer losses are not significant for low and moderate current densities if the flow field is appropriate for gas removal. Thus, the mass transfer overpotentials can be neglected for up to 3 A/cm², [5].
- Activation losses are dominant at low current densities, while the ohmic overpotential becomes dominant at mid current densities [5].
- Pressure and Temperature is kept constant. This is normal in practice

Figure 3 shows the reduced equivalent circuit made up of a series connection of a resistance (mainly due to ohmic losses) and a fixed voltage source (the open circuit voltage). The value of this resistance can be estimated from the slope of the I-V curve between the boundaries of upper and lower operating current densities for a given cell area. It must be noted that larger scale electrolyzer units are made up of an aggregation of smaller units (1 to 2 MW) connected in parallel and operating at medium current densities [9], therefore the above simplification assumptions hold for larger systems. The simplified PEM stack model is implemented in RSCAD with **rtids_vsc_BRC3** library model. The open cell voltage is set using the "CC Word" parameter in the settings for the voltage source. This variable can be changed to reflect open cell voltage at different operating temperature and pressure.

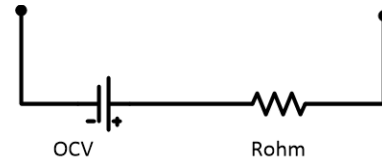


Fig 3: Reduced equivalent circuit of PEM stack implemented in RSCAD.

I. POWER CONVERSION SYSTEM AND REPRESENTATIONS IN RSCAD

The amount of gas produced by an electrochemical process is related to the electrical charge consumed by the cell. This relationship is described by Faraday's law in (10).

$$m = (Q/F) \cdot (M/z) \quad (10)$$

Where m is the mass of the substance generated at an electrode in grams, Q is the total electric charge passed through the substance in coulombs, $F = 96500$ [Coulombs per mol] is the Faraday constant, M is the molar mass of the substance in grams per mol, and z is the valency number of ions of the substance (number of electrons transferred). Under ideal conditions, the electric charge, passing through the electrolysis cell, is directly related to the amount of hydrogen and oxygen produced. For each mole of hydrogen produced, two electrons circulate through the external circuit. It is also known that

$$Q = I \cdot t \quad (11)$$

By rearranging terms of (10) and substituting in Q from (11) we obtain hydrogen output per unit time (kg per second)

$$H_{2out} = M / (2 \cdot F) * I \quad (12)$$

It can be seen from (12) that the hydrogen output is directly proportional to the current fed to the electrolysis cell or stack. Therefore in order to control hydrogen generation

output (which is the primary function of the Power to Gas plant) the current to the stack must be precisely controlled. Therefore in order to control the total demand of the electrolyser, the stack current is the main control variable. The typical configuration of the power conversion system is shown in figure 4. The AC-DC and DC-DC conversions are implemented in a number of ways by different manufacturers. The generic RSCAD model allows the rectifier stage to be configured as diode rectifier or as an Active Front End converter. In this paper, the AC-DC conversion is implemented with a 3-phase diode rectifier followed by a DC-DC converter for simplicity of control [11]. The control of current to the cell/stack is done with a DC-DC converter (i.e. configured as buck converter).

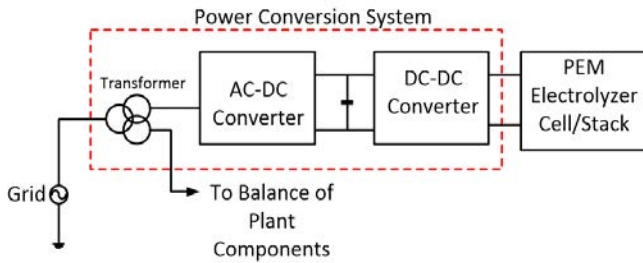


Fig 4: Components of power conversion system (controls not shown)

E. Load Current control with DC-DC converter

The current fed into the electrolyzer stack is controlled via the DC-DC converter. The model assumes average current mode (ACM) control. ACM control has several advantages over peak current control such as the elimination of the external compensation ramp, increased gain for current loop at low frequency range and improved immunity to noise in the sensed current signal [10]. The average current mode control is also used in multiphase DC/DC converters to ensure accurate current sharing among phases [10]. It is however unable to provide peak switch current limiting. For high current applications which require low output current ripple the interleaved mode of operation is used. With this approach additional switch network pairs (diode and switching device) are added with output inductors which are connected in parallel to share a common output capacitor and load. In this model, multiple-cell buck converter topology is adopted; the cells are switched with the same duty ratio, but with a relative phase shift introduced between each cell in order to reduce the magnitude of the output ripple at the output of the converter. With this approach it has been demonstrated that the output ripple is reduced [12]. The model has added flexibility of switching off the additional cells where interleaved operation is not required. In practice two or more DC-DC converters are connected in parallel to realize high output currents. The firing pulses for the switches are derived from comparing a control voltage signal (from a PI controller) to a sawtooth waveform as shown in figure 6. The control voltage signal is generated by passing an error signal generated by comparing stack current to a load reference, through a PI controller.

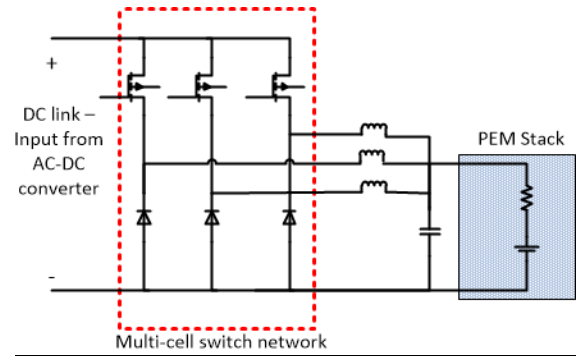


Fig 5: Multi-cell buck converter implementation in RSCAD.

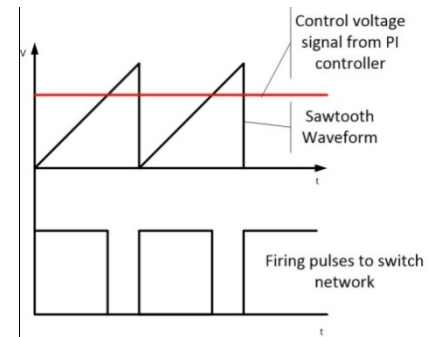


Fig 6: Firing pulses derived from comparing PI controller output to a sawtooth waveform.

The PWM comparator is implemented with a firing pulse generator (`rtids_vsc_3LGFIR`). The saw tooth waveform from the generator (`rtids_vsc_TRIWAV3`) is compared with the output of the PI compensator to generate firing pulses for the switches in the DC-DC converter. The load current reference signal is the control input. K_m is the PWM modulator gain, $G_c(s)$ is the PI compensator transfer function. $G_i(s)$ is the duty ratio to output current transfer function and $H(s)$ the sensor transfer function.

F. AC-DC rectifier

This paper assumes an uncontrolled AC-DC converter for simplicity. The limitation with this model is the possible variations in DC link voltage with voltage disturbances on the AC side of the converter; however this study assumes a balanced steady state AC voltage input to the rectifier. The uncontrolled rectifier is implemented in RSCAD with two level VSC library models (`rtids_vsc_LEV2`) with the firing pulse set to zero. The parallel rectifiers are fed from a phase shift transformer are connected in parallel. The 30° phase shift facilitates cancellation of harmonics which leads to a reduction in total harmonic distortion [18]. The power conversion system is implemented in the small time step domain within a VSC bridge box. The small time step model of the rectifier (and DC-DC converter) allows export and import of real signals (example firing pulses) from external hardware (e.g. Control Hardware in the Loop).

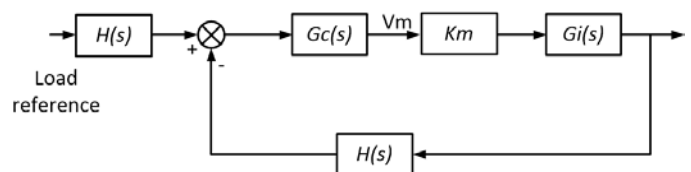


Fig 7: functional block diagram of current control loop

G. Transformer Model

The model of the grid transformer can vary depending on winding configuration used in the application. In the generic model, a three winding transformer (delta primary and wye secondary windings) is assumed. The model assumes magnetizing branch current of 1% of rated current and positive sequence leakage reactance of 6% for all windings. This is in line with typical values for large transformers [13]. The grid transformer is implemented with a library model (rtds_3P3W_TRF) of a three phase three winding transformer as shown in fig 10.

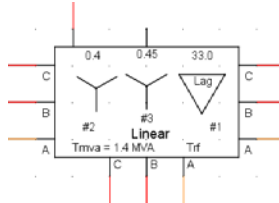


Fig 10: Three-winding transformer library model in RSCAD

II. BALANCE OF PLANT MODEL AND REPRESENTATION IN RSCAD

The operation of a PEM stack is only possible with additional components and subsystems [5]. In order to capture the full electrical response it is important to model these additional components which are collectively known as Balance of Plant. To model balance of plant components, a simple load model which has similar characteristics to the detailed load model is chosen. The sum of all power inputs to the electrolyser is given by (13)

$$P_{electrolyser} = P_{AC} + P_{BOP} \quad (13)$$

Where the electrical power supplied to the rectifier is P_{AC} and P_{BOP} is power consumed by balance of plant components which includes circulation pumps. The aggregated electrical response of the balance of plant components is assumed to be constant. This assumption is based on the view that most of the electronics loads such as control systems etc. have a fixed consumption. Secondly, the circulation pump is assumed to work continuously. This is based on the fact that the electrolyser is operated with forced convection in order enhance water transport to, and gas removal from the electrodes. This ensures a low temperature gradient over the stack [5]. The formation of bubbles at the electrode along with its attendant problems are avoided with this mode of operation. According to [14] the electrical power required by a pump as a function of capacity, pressure and efficiency is expressed by (12)

$$P_{pump} = \frac{Q \cdot \Delta p}{36 \cdot \eta} \quad (12)$$

Where P_{pump} is the electrical power input to the motor, Q is the pump capacity in cubic meters per hour, Δp the pressure differential in bars and η is the combined efficiency of the motor, transmission and pump. Assuming a steady flow of water at a fixed pressure differential and a fixed efficiency, it can be observed that the power consumption is fixed. Taking this assumption and neglecting power consumption of other components, the aggregated Balance of Plant can

be represented fairly accurately by a static load. The static load model expresses the characteristic of the load at any instant of time as algebraic functions of the bus voltage magnitude and frequency [9].

$$P = P_0 * (V')^a \quad (13)$$

$$Q = Q_0 * (V')^b \quad (14)$$

$$V' = \frac{V}{V_0} \quad (15)$$

Where P and Q are active and reactive components of the load. P_0 and Q_0 represent initial values of P and Q . The parameters a and b are set at 0 to represent constant power loads. In practice Balance of plant components are fed from a separate AC supply and operate at steady state and are therefore not impacted by the demand set point changes sent to the electrolyser. The implementation of the BoP is done with a dynamic load model library component within RSCAD (rtds_udc_DYLOAD).

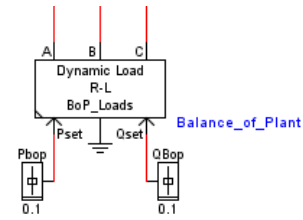


Fig. 11: Balance of Plant loads model implementation in RSCAD

The load parameter is set with sliders which can be varied during the simulation. This flexibility exists within the model to allow simulation of changes in BoP load power consumption in real time.

III. MODEL PERFORMANCE

The performance of the model is tested with a simple network comprising a source, transmission line, transformer and electrolyser. The network is adequate for analyzing response of the model to step changes in load current set points. The simple network shown in fig 12 comprises an 110kV source which represents the infinite grid connected to the 33kV rated load (electrolyser) via a transmission line and step-down transformer. By tuning the parameters, the response of the real electrolyzers can be reproduced in the simulation with a good level of accuracy. It must also be noted that performance can be modified to approximate response of different models of electrolyzers by simply adjusting the parameters of the controller.

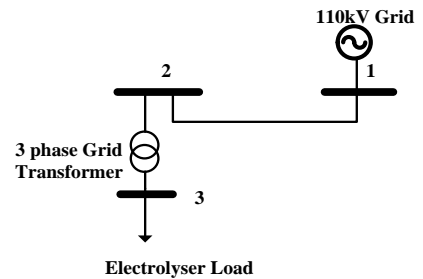


Fig. 12: Test system showing electrolyzer connection to 110kV infinite grid via step down transformer.

H. Ramp up – Load current step change from 10% to 100%

From (12) it can be seen that an increase hydrogen production requires an upward adjustment of current fed to the stack. This leads to an increase in active power drawn from the grid as well. This is the basic operating principle used to store excess generated energy as hydrogen gas. Thus electrolyzers configured to increase demand and hydrogen output based on a signal from a high level controller or dispatch center must be able to ramp up demand within a certain time frame. The model is capable of emulating the response of an electrolyzer whose stack current set point has been adjusted upward via a step command. Fig 13 and 14 show the response to the step change for stack current and active power demand respectively. This command is typically initiated by a user from a control panel, the grid dispatch center or from a high level controller. The electrolyzer responds by adjusting the current fed to the stack in less than 2 seconds. This response can be tuned to model the response of a variety of electrolyzers.

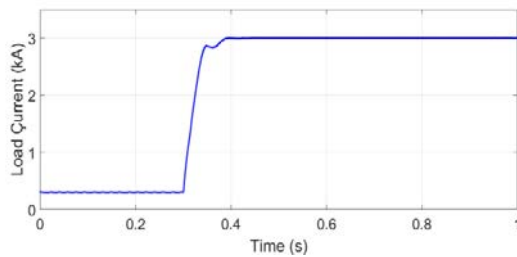


Fig. 13: Response of electrolyzer to load current set point increase.

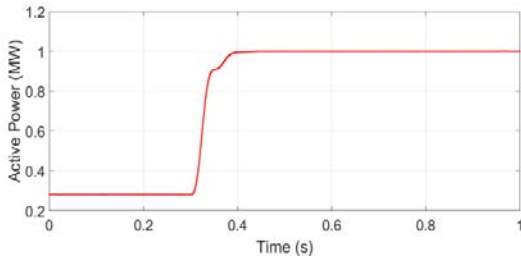


Fig. 14: Active power response to load set point increase

I. Ramp down – Load current step change from 100% to 10%

Figure 15 shows the response of the model to a step decrease in load current setpoint. It can be seen that the response is less than 2 seconds. This feature is particularly of interest in frequency containment reserve (FCR) applications in future grids since electrolyzers are known to have relatively faster response compared to generator governors [16]. The fast response time characteristics also holds potential for improving nadir frequency after a disturbance.

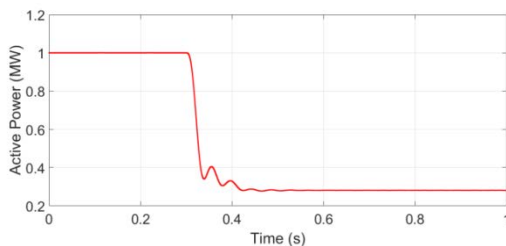


Fig. 15: Active Power response of electrolyzer to load current set point decrease.

IV. MODEL SCALING APPROACH

In practice large scale electrolyzers in the range of >5MW are an aggregation of smaller basic blocks which range from 1 to 2MW connected in parallel [9]. This principle is adopted in scaling the RSCAD model. In the model it is assumed that there are no interactions between the controllers of the various sub units and all controllers respond simultaneously to the same input command. Therefore by the principle of superposition, N units of 1MW electrolyzers will provide N MW total demand. Scaling of the electrolyzer model can be achieved by setting the scaling parameters (enscl, scupr, namsc, sclwr, scini) of the VSC interface transformer model (Rtds_vsc_IFCTR1) in the RSCAD component library. Fig 16 shows the response of the model scaled to produce a demand of 300MW.

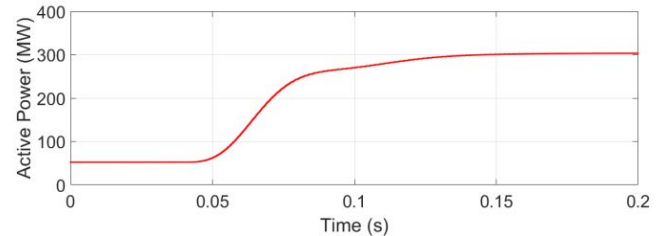


Fig 16: Active Power demand of scaled model of electrolyzer (300MW).

J. Comparison with Real Electrolyzer response

Obtaining real data from a large scale electrolyzer for model verification has been a challenge mainly due to difficulty in accessing proprietary information. However; some data has been obtained from published literature on smaller sized electrolyzers. For purposes of demonstrating similarities in demand profile, the model verification is done with the available data. Figures 17 and 18 show the response of a real PEM electrolyzer to set point step changes. Comparing figures 13 and 17 for example, it can be seen that the response profile of the real electrolyzer is similar to that of the RSCAD model.

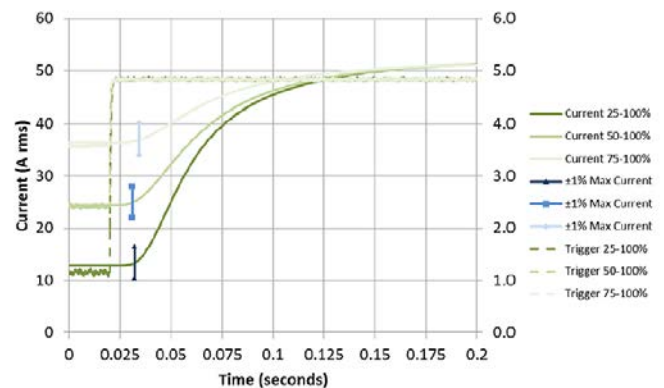


Fig 17: Load current response to set point increase for real PEM electrolyzer. Extracted from [16]

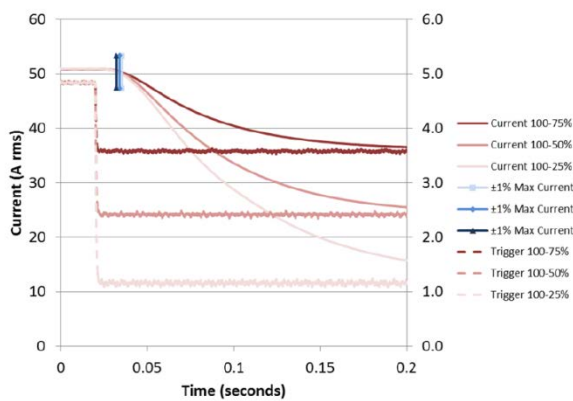


Fig 18: Load current response to set point increase for a real PEM electrolyser. Extracted from [16]

V. CONCLUSIONS

Proton Exchange Membrane (PEM) electrolysers hold significant promise as the preferred technology for large scale electrolysers. Understanding interactions of large scale PEM electrolysers with the other sources of ancillary services is crucial within the context of the multi-energy system. Generic models of large scale PEM electrolysers (>1MW) for real time digital simulation will be a valuable tool in the study of new sources of ancillary services for the electrical power system. As the number of large scale electrolysers is projected to grow exponentially, these models will significantly enhance the understanding of potential effects of integrating large scale electrolysers into the power grid. This paper demonstrates the feasibility of creating such generic large scale models. The results from a case study built on a MW-scale plant connected to an infinite grid, appear to support the view that a generic scalable model of large scale electrolysers in RTDS is feasible. The generic model captures the key subsystems of large scale electrolysers, namely the PEM stack, power conversion and balance of plant. The model has features which enables flexible adaptation and scaling to replicate the electrical response of various capacities (up to hundreds of MW) of PEM electrolysers. The added value large scale electrolysers can bring to ancillary services provision in the power system is linked mainly to their fast reaction time and large energy storage capabilities. However, leveraging additional capabilities of large scale electrolysers for ancillary services to the power system will require additional functions, i.e. addition of front end controllers (FEC). Future research is aimed at extending the generic model in RSCAD to include the FEC. The extended model will facilitate comprehensive study of dynamic interactions of large scale electrolysers with other sources of ancillary services.

VI. ACKNOWLEDGEMENT



Co-financed by the European Union
Connecting Europe Facility



This work has received funding from the European Union's Connecting Europe Facility

(CEF) programme under the grant agreement No INEA/CEF/SYN/A2016/1336043 – TSO2020 Project (Electric “Transmission and Storage Options” along TEN-E and TEN T corridors for 2020). This paper reflects only the authors’ views and the European Commission is not responsible for any use that may be made of the information it contains.

REFERENCES

- [1] V. Suárez, P. Ayivor, J. Torres, and M.A.M.M. van der Meijden. “Demand Side Response in Multi-Energy Sustainable Systems to Support Power System Stability”, presented at 16th Wind Integration Workshop, Berlin, Germany, 2017.
- [2] www.noordelijkeinnovatieboard.nl (2017). *The Green Hydrogen Economy in the Northern Netherlands* [Online]. Available: <http://verslag.noordelijkeinnovatieboard.nl/download/aden-als-pdf>. [Accessed Aug 10, 2017].
- [3] Harvey, R., Abouatallah, R., & Cargnelli, J., “Large-scale water electrolysis for power-to-gas”, in *PEM Electrolysis for Hydrogen Production: Principles and Applications*, 2016, pp. 303-313.
- [4] Ruuskanen, V., Koponen, J., Huoman, K., Kosonen, A., Niemelä, M., & Ahola, “PEM water electrolyzer model for a power-hardware-in-loop simulator”. *International Journal of Hydrogen Energy*, vol. 42, no.16, pp.10775-10784, 2017.
- [5] Smolinka, T., Ojong, E. T., & Lickert, T., “Fundamentals of PEM water electrolysis”, in *PEM Electrolysis for Hydrogen Production: Principles and Applications*, 2016, pp.11-33.
- [6] Der Merwe, V., & Petrus, J. H., “Characterization of a proton exchange membrane electrolyser using electrochemical impedance spectroscopy”, Doctoral dissertation, North-West University, USA, 2012.
- [7] Millet, P., “Characterization Tools for Polymer Electrolyte Membrane (PEM) Water Electrolysers”, in *PEM Electrolysis for Hydrogen Production: Principles and Applications*, 2016, pp.179.
- [8] Da Costa Lopes, F., & Watanabe, E. H., “Experimental and theoretical development of a PEM electrolyzer model applied to energy storage systems”, In *Power Electronics Conference, 2009. COBEP'09, 2009*, pp. 775-782.
- [9] Simon Bourne, “Scaling PEM Electrolysis To 100MW”, [Online]. Available: <https://www.h2fc-fair.com/hm17/images/forum/tf/2017-04-25-1100.pdf> [Accessed Feb 9 2018].
- [10] Yanfei, L. I. U., “A unified large signal and small signal model for DC/DC converters with average current control”. *Transactions of china electrotechnical society*, vol.22, no.5, pp. 84-91, 2007.
- [11] Solanki, J., Frohliche, N., Bocker, J., & Wallmeier, P. (2013). Comparison of thyristor-rectifier with hybrid filter and chopper-rectifier for high-power, high-current application. In *Proc. PCIM Europe*, 2013.
- [12] Shrud, M. A., Kharaz, A. H., Ashur, A. S., Faris, A., & Benamar, M., “Analysis and simulation of automotive interleaved buck converter”. *World academy of science, engineering and technology*, 2010.
- [13] Teshmont Consultants, L. P., & Karim, S, *Transformer Modeling Guide*, AESO, Alberta Electric System Operator, Revision, 2014.
- [14] Vogelesang, H., “An introduction to energy consumption in pumps”, *World pumps*, vol.2008, no.496, pp. 28-31, 2008.
- [15] P. Kundur, “Power System Loads”, in *Power System Stability and Control*, McGraw-Hill, 1994, pp. 293-313.
- [16] J. Eichmann, K. Harrison and M. Peters, “Novel Electrolyser Applications: Providing More Than Just Hydrogen,” National Renewable Energy Laboratory, Denver, CO, Technical Report NREL/TP-5400-61758, Sep. 2014.
- [17] Lebbal, M. E., & Lecœuche, S., “Identification and monitoring of a PEM electrolyser based on dynamical modeling”. *International journal of hydrogen energy*, vol. 34, no. 14, pp.5992-5999, 2009.
- [18] Wu, B., & Narimani, M., *High-power converters and AC drives* (Vol. 59). John Wiley & Sons, 2017.